Research on Engineering Structures & Materials
www.jresm.org
Research Group

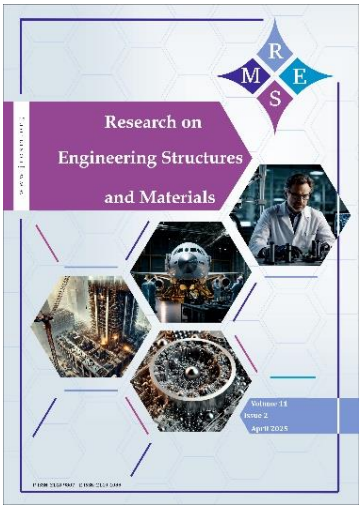

Experimental evaluation of bond behavior of post-installed GFRP and steel reinforcements using different adhesives

Borkan M. Mutashar, Suhaib Y. Kasim, Oday A. Salih

Online Publication Date: 30 December 2025

URL: http://www.jresm.org/archive/resm2026-1246ic1012rs.html
DOI: http://dx.doi.org/10.17515/resm2026-1246ic1012rs

Journal Abbreviation: *Res. Eng. Struct. Mater.*

To cite this article
Mutashar B M, Kasim S Y, Salih O A. Experimental evaluation of bond behavior of post-installed GFRP and steel reinforcements using different adhesives. *Res. Eng. Struct. Mater.*, 2026; 12(2): 1055-1066

Research on Engineering Structures & Materials
www.jresm.org
Research Group

Research Article

Experimental evaluation of bond behavior of post-installed GFRP and steel reinforcements using different adhesives

Borkan M. Mutashar [*,1,2,a], Suhaib Y. Kasim [1,b], Oday A. Salih [1,c]

[1]*Department of Civil Engineering, University of Mosul, Mosul, Iraq*
[2]*Department of Environmental Technologies, University of Mosul, Mosul, Iraq*

Article Info

Article History:

Received 12 Oct 2025
Accepted 27 Dec 2025

Keywords:

Bond strength;
GFRP bars;
Post-installed Reinforcement;
Adhesive anchoring,
Pull-out test;
Embedded length

Abstract

The existing design codes lack specifications for the use of glass fiber-reinforced polymer (GFRP) bars in post-installation applications, and research on this topic is scarce. This study investigates the bond performance of the post-installed GFRP and steel reinforcement bars through pull-out tests using three commercial chemical adhesives. Seventy cylindrical specimens (60 post-installed, 10 cast-in-place) with diameters of 15 cm and heights of 30 cm were prepared. Post-installed samples featured anchor bars with 5d, 10d, and 15d embedded lengths (where d is the rebar diameter), tested under dry and wet conditions. Compressive strengths of 25 MPa and 35 MPa were used. Three different commercial adhesive types were utilized in this research: pure epoxy adhesive (adhesive A) and two epoxy acrylate adhesives (adhesives B and C). Adhesive A demonstrated improved bond strength by up to 75% with longer embedded lengths and higher concrete compressive strengths when compared to adhesives B and C, regardless of moisture conditions. All specimens showed concrete rupture or splitting failure, proving the effectiveness of the epoxy resins as bonding agents. The findings emphasize the significance of adhesive selection and design parameters in improving bond performance.

1. Introduction

Post-installed reinforcement of steel represents a reliable retrofitting and strengthening technique. Steel reinforcing bars, on the other hand, tend to suffer from corrosion, which results in costly maintenance and repairs [1]. These issues have motivated researchers to explore alternative reinforcing materials with enhanced durability. As an alternative to steel, Glass Fiber Reinforced Polymer (GFRP) reinforcement bars are corrosion-resistant, characterized by their lighter weight, and have a higher tensile strength-to-weight ratio [2]. This highlights the need for a comprehensive research effort directed towards future codification, given that previous studies, along with design codes like ACI440, do not provide experimental data to support post-installed GFRP reinforcing bars; they focused only on the cast-in GFRP bars. Consequently, there is still a lack of knowledge regarding the structural performance and anchoring reliability of post-installed GFRP reinforcement.

Bonded anchors that are installed in concrete to serve as structural connections can be categorized into two types: cast-in-place anchors and post-installed anchors in concrete [3-5]. The post-installed reinforcement is added to an existing concrete segment by drilling holes and injecting adhesives. [6]. This approach is employed for various functions, including connecting newly constructed concrete to existing or previously constructed concrete, facilitating continuity and uniform stress transfer [7]. These bars are usually glued or mortared into a pre-drilled hole [8].

*Corresponding author: borkan.22enp20@student.uomosul.edu.iq
[a]orcid.org/ 0009-0009-5019-373X; [b]orcid.org/0000-0001-5346-8836; [c]orcid.org/0000-0002-2882-8622
DOI: http://dx.doi.org/10.17515/resm2026-1246ic1012rs

It is widely recognized that load or stress distribution in reinforced concrete members is influenced by the bond within the reinforcement and the concrete or binder surrounding it [9]. This transfer can be achieved by the opposition to the relative movement or the slipping between the concrete and the bar's rib edges [10]. Bond strength, or resistance to slipping, is determined by three actions: The bar's ribs bond with the surrounding concrete through friction, mechanical connection, and chemical adhesion [11]. Bond performance must be assessed to determine the best anchoring for every application. The failure mechanisms, pull-out loads, and load displacement of different anchor types are included [12].

Previous investigations focused on cast-in-place GFRP bar bond strength [13-15]. After being inserted into concrete as post-installed reinforcement, their bonding performance may differ completely, due to the installation conditions. The effect of factors, including concrete compressive strength, environmental conditions, and epoxy adhesive performance with different embedding lengths, on post-installed GFRP bars has not been studied. Therefore, a thorough comparison of the bond behavior of post-installed steel and GFRP bars bonded with locally available different adhesive types is essential to enhance the effectiveness and reliability of retrofitted structures. The purpose of this study is to examine the performance of steel and GFRP anchors that have been post-installed using various construction adhesives in pull-out tests. This study examined how embedded lengths affected pull-out loads in concrete specimens with post-installed and cast-in-place rebar. This research will help Iraqi infrastructure projects with rehabilitation throughout construction be more structurally durable.

2. Materials and Mixing

2.1. Cement

The type of cement selected in this research is ordinary Portland cement from the Mass Cement Factory in Sulaymaniyah Governorate. In a laboratory-controlled room with an ambient temperature of 24 °C, along with a relative humidity (RH) of 42%, the properties of the cement were determined, as shown in Table 1.

Table 1. Physical properties of cement

No.	Characteristics	Units	Value	Specification
1	Standard Consistency w/c	-	0.31	
2	Initial setting	Minutes	115	≥ 45
3	Final setting	Minutes	235	≤ 600
4	Compressive strength (3 days)	MPa	22.1	≥ 15
5	Compressive strength (7 days)	MPa	31.2	≥ 23
6	Fineness (sieve no. 170)	%	4	≤ 10

2.2. Reinforcing Bars

The mechanical properties of GFRP and steel rebars were tested using a Universal Testing Machine (UTM) with 1000 kN capacity, in accordance with ASTM A706 [16]. A total of three rebar samples of each rebar type were tested to ensure comprehensive results; their mechanical properties were calculated as the averages of their respective values. The GFRP bars employed in this study are 12 mm in diameter, type No. B80 – Epoxy Resin, supplied by Jiangsu Feibol China, and its properties are described in Table 2. The steel bars employed in this study are 12 mm in diameter, provided by Mass Steel Factory in Sulaymaniyah Governorate, Iraq. The characteristics of these bars are presented in Table 3.

Table 2. Properties of GFRP bars

Bar Diameter (mm)	Ultimate Tensile Strength (MPa)	Elongation	Weight (g/m)
12	900	1.3%	240

Table 3. Properties of steel bars

Bar Diameter (mm)	Yield Stress (MPa)	Ultimate (MPa)	Elongation	Weight (g/m)
12	463	696	16.2%	890

2.3 Concrete Mix

Cement, water, and local river round coarse and fine aggregate from Kanhaash near Mosul make up the concrete mixtures. This study used a maximum size of 14 mm coarse aggregate and 3.9 mm for sand. ASTM measured aggregate properties. ASTM C127 [1] and C128 [2] measured aggregate absorption and specific gravity, while ASTM C29 [3] measured compact and lose weight. Sieve analysis fulfilled the ASTM C136 standards [4]. Two distinct concrete mixes with varying concrete strengths were created to establish a comparison investigation. The chosen concrete strengths of the research are 25 and 35 MPa, since they are the most prevalent strengths in actual constructions. The mix was designed in line with ACI 211.1 standards [5]. The proposed w/c ratios to provide 25 and 35 MPa concrete compressive strength were held constant at 0.41 and 0.39, respectively. Table 4 summarizes the combined proportions of components. The concrete compression machine was used for testing the concrete cylinders. Three concrete cylinders had respective compressive strengths of 24.9, 25.3, and 26 MPa for C25, and another three cylinders with the compressive strengths of 34.1, 35.5, and 36.3 MPa for C35.

Table 4. Material mix proportions per cubic meter

Batch No	Batch Code	Cement (kg)	Coarse aggregate (kg)	Fine aggregate (kg)
1	C25	350	977	695
2	C35	400	981	629

2.4 Adhesives

Three different commercial adhesive types commonly used in Iraqi infrastructure were utilized.

- Adhesive A: Adhesive A is a two-part, thixotropic fixing adhesive containing epoxy resin that can be employed for anchoring deformed bolts and reinforcement bars in dry or wet concrete holes. The technical properties of the adhesive are shown in Table 5.
- Adhesive B: Adhesive B is a two-part, high-performance fixing adhesive containing epoxy acrylate, free from solvents and styrene. The properties of the adhesive are shown in Table 6.
- Adhesive C: Adhesive C is a high-resilience, rapid curing, styrene-free, containing acrylate resin anchoring grout provided in a pre-packaged cartridge system and it may be used on many surfaces. Table 7 illustrates the properties of the adhesive.

Table 5. Properties of adhesive A

Description	Sample Results	
Compressive strength	95 MPa (7 days, +20°C)	
Tensile Strength in Flexure	45 MPa (7 days, +20°C)	
Tensile Strength	23 MPa (7 days, +20°C)	
Modulus of Elasticity in Tension	5500 MPa (7 days, +20°C)	
Service Temperature	Long term	-40 °C min. / +50 °C max.
	Short-term (1–2 hours)	+70 °C

Table 6. Properties of adhesive B

Description	Sample Results
Compressive strength	68 MPa (7 days, +20°C)
Tensile Strength in Flexure	24 MPa (7 days, +20°C)

Tensile Strength	13 MPa (7 days, +20°C)	
Modulus of Elasticity in Tension	3700 MPa (7 days, +20°C)	
Service Temperature	Long term	-40°C min. / +50°C max.
	Short-term (1–2 hours)	+70°C

Table 7. Properties of adhesive C

Description	Sample Results	
Compressive strength	75 MPa (7 days, +20°C)	
Tensile Strength in Flexure	25 MPa (7 days, +20°C)	
Tensile Strength	12 MPa (7 days, +20°C)	
Modulus of Elasticity in Tension	3500 MPa (7 days, +20°C)	
Service Temperature	Long term	-40 °C min. / +50°C max.
	Short-term (1–2 hours)	+65°C

3. Dimensions and Testing Procedure

The experimental setup includes a pull-out test to assess the strength of adhesives used to adhere GFRP reinforcement. To guarantee reliability and statistical assessment of the results, every test setup has been duplicated twice. Concrete cylinders with a diameter of 15 cm and a height of 30 cm were utilized for post-installed reinforcement bars into concrete, whereas 10 cast-in-place specimens were utilized as controls. Hardened concrete cylinder samples were drilled for 60 post-installed rebar concrete specimens comprising the various test parameters that include bar material (steel and GFRP), embedded lengths of 5, 10, and 15 with rebar diameters (5Ø, 10Ø, and 15Ø), varying hole surface conditions (dry and wet, indicating the moisture status inside the drilled hole prior to adhesive application), concrete compressive strength 25 MPa and 35 MPa, and three different epoxy-based adhesives (adhesive A, adhesive B and adhesive C) were used to create the bond.

The flowchart for the experimental procedure (Fig. 1) describes the experimental process flowchart. The pull-out value recorded was the average of two replicas. Specimen names were coded through six symbols that denoted test parameters. The arrangement of these symbols is as follows: method of installation (C for cast in place and P for post-installed), concrete compressive strength (C_{25} for 25 MPa and C_{35} for 35 MPa), bar type (G for GFRP and S for Steel), embedded lengths ($5d_b$, $10d_b$ and $15d_b$ mm.) where d_b is bar's diameter, drilled hole surface condition (D for dry and W for wet), and the adhesives (AA for adhesive A, AB for adhesive B and AC for adhesive C). For example, P-C_{35}-G-$10d_b$-D-AC is a specimen with 35 MPa compressive strength, post-installed GFRP bars, a $15d_b$ embedment length, a dry hole surface, and adhesive C.

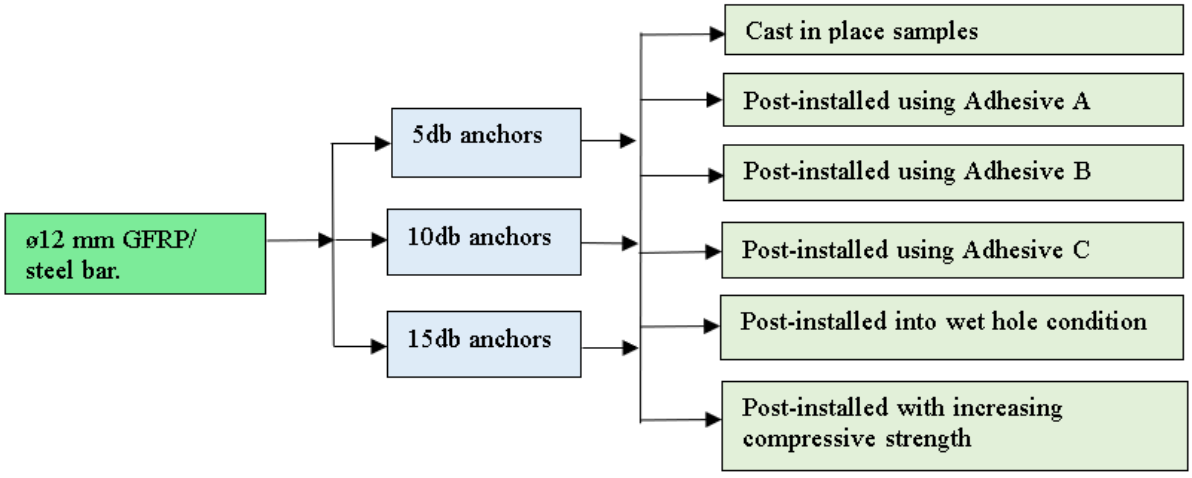

Fig. 1. Experimental program flow chart

3.1 Mixing, Casting, and Curing Procedures

The constituent materials of the concrete were accurately proportioned, weighted, and subsequently mixed in a rotary mixer. Three equally sized layers of freshly mixed concrete were poured into the cylindrical molds measuring 15 cm by 30 cm. According to ASTM C192, the concrete test specimens were demolded and cured for a week under water ponding for 24 hours. The specimens were exposed to air and allowed to dry for three more weeks before the drilling operation started [20]. in this study, the anchoring lengths or embedment depths employed were five, ten, and fifteen times the bar diameter.

3.2 Drilling, Cleaning, and Injecting of The Holes

The concrete cylinder specimens with post-installed rebar were drilled across the specimens' longitudinal axis to form holes using a vibrating rotary hammer drill with chrome alloy steel shank bits of 16 mm. The drill bits were marked to get the desired embedment lengths. Additionally, a drill stand was used to ensure the verticality of bars. All loose concrete particles that would interfere with the rebar's ability to bond effectively with the concrete were eliminated using a wire brush along with an air compressor, as seen in (Fig. 2). In order to simulate the real-world practical scenarios, two-hole conditions free of moisture and a moisture-retained surface were assessed in this investigation. Once the cleaning was completed, adhesives were applied into the holes, and GFRP bars of 1300 mm were subsequently installed according to ASTM 440.3 [22]. Adhesives were poured into the holes using an adhesive injection gun. The adhesive injection process, which involves combining mortar with a curing agent, started at the bottom of the hole and continued until two-thirds of the hole's volume was filled. The curing time and adhesives preparation process were selected according to the manufacturer's recommendations. The bars were carefully aligned at the center of the hole with constant twisting to provide an even layer of adhesive over the bar. The bars were properly positioned before the adhesive began to set. All of the post-installed bars were left undisturbed for 24 hours at 25°C to ensure the adhesive was fully cured under identical conditions.

3.3 Achor Preparation for Gripping GFRP Bars

GFRP bars were secured tightly to prevent breakage and guarantee exact results. The anchors for the GFRP bars were made by using steel tubes filled with two-part epoxy adhesive according to ASTM 440.3R [22]. Specimens are tested following a three-day curing period of the two-part epoxy adhesive (Sikadur-31), as illustrated in (Fig. 3).

Fig. 2. Drilling and cleaning of the holes

Fig. 3. GFRP bar anchor

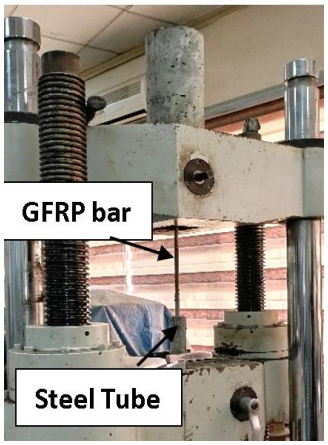

Fig. 4. Pull-out test setup in UTM

4. Results and Discussion

Pull-out tests were conducted on reinforcing bars installed in concrete cylinders to investigate the tensile strength of adhesives, as illustrated in (Fig. 4). The bond stress between the post-installed rebars and the surrounding concrete is assumed to be equally distributed along the embedment length. The bond strength can be calculated by utilizing Eq (1):

$$\tau = \frac{P_{max}}{\pi d_b l_e}. \quad (1)$$

In this equation, τ refers to the average bond strength measured in MPa, P_{max} represents the peak pull-out load in kN, d_b indicates the diameter of the reinforcing bar in mm, and *le* represents the embedment length in mm. The calculated average bond strength values for the different specimen sets are presented in Table 8.

Table 8. The average values of the bond strength and the pull-out loads

No.	Name	Pull-out load (kN)	Standard deviation (kN)	Average pull-out load (kN)	Average bond strength (MPa)
	P-C_{25}-G-5d_b-D-AA	22.19	0.14	22.09	9.770878
	P-C_{25}-G-5d_b -D- AA	21.99			
	P-C_{25}-G-10d_b-D-AA	35.13	2.03	33.10	7.320418
	P-C_{25}-G-10d_b-D-AA	31.07			
	P-C_{25}-G-15d_b-D-AA	52.04	1.17	50.87	7.500295
	P-C_{25}-G-15d_b-D-AA	49.70			
	P-C_{25}-G-10d_b-W-AA	30.47	1.34	29.13	6.44241
	P-C_{25}-G-10d_b-W-AA	27.79			
	P-C_{35}-G-10d_b-D-AA	40.03	0.71	39.53	8.742481
	P-C_{35}-G-10d_b-D-AA	39.03			
	P-C_{25}-S-5d_b-D-AA	23.99	1.38	23.01	10.17781
	P-C_{25}-S-5d_b-D-AA	22.03			
	P-C_{25}-S-10d_b-D-AA	35.12	1.17	35.95	7.950725
	P-C_{25}-S-10d_b-D-AA	36.77			
	P-C_{25}-S-15d_b-D-AA	54.17	1.31	53.24	7.849729
	P-C_{25}-S-15d_b-D-AA	52.31			
	P-C_{25}-S-10d_b-W-AA	31.95	0.45	31.63	6.995311
	P-C_{25}-S-10d_b-W-AA	31.31			
	P-C_{35}-S-10d_b-D-AA	44.67	0.59	44.25	9.786359
	P-C_{35}-S-10d_b-D-AA	43.83			
	P-C_{25}-G-5d_b-D-AB	21.67	0.23	21.51	9.514331
	P-C_{25}-G-5d_b-D-AB	21.35			

P-C_{25}-G-10d_b-D-AB	28.01	0.38	27.74	6.134996
P-C_{25}-G-10d_b-D-AB	27.47			
P-C_{25}-G-15d_b-D-AB	36.66	1.60	35.50	3.526775
P-C_{25}-G-15d_b-D-AB	34.39			
P-C_{25}-G-10d_b-W-AB	24.11	0.27	23.92	7.851203
P-C_{25}-G-10d_b-W-AB	23.73			
P-C_{25}-G-10d_b-D-AB	31.74	1.34	30.79	6.809536
P-C_{25}-G-10d_b-D-AB	29.84			
P-C_{25}-S-10d_b-D-AB	22.17	0.44	21.86	9.669144
P-C_{25}-S-5d_b-D-AB	21.55			
P-C_{25}-S-10d_b-D-AB	28.45	1.86	29.77	6.583953
P-C_{25}-S-10d_b-D-AB	31.08			
P-C_{25}-S-15d_b -D-AB	40.47	1.02	39.75	5.860757
P-C_{25}-S-15d_b-D-AB	39.03			
P-C_{25}-S-10d_b-W-AB	25.97	0.52	25.60	5.661713
P-C_{25}-S-10d_b-W-AB	25.23			
P-C_{35}-S-10d_b-D-AB	33.03	1.16	33.85	7.486288
P-C_{35}-S-10d_b-D-AB	34.67			
P-C_{25}-G-10d_b-D-AC	13.4	1.23	15.74	6.962137
P-C_{25}-G-5d_b-D-AC	15.14			
P-C_{25}-G-10d_b-D-AC	24.91	0.29	24.71	5.46488
P-C_{25}-G-10d_b-D-AC	24.50			
P-C_{25}-G-15d_b-D-AC	31.05	2.15	29.02	3.022529
P-C_{25}-G-15d_b-D-AC	26.99			
P-C_{25}-G-10d_b-W-AC	21.01	0.72	20.50	6.418082
P-C_{25}-G-10d_b-W-AC	19.99			
P-C_{35}-G-10d_b-D-AC	28.03	2.84	26.02	5.7546
P-C_{35}-G-10d_b-D-AC	24.01			
P-C_{25}-S-5d_b-D-AC	16.90	1.13	16.10	7.121373
P-C_{25}-S-5d_b-D-AC	15.30			
P-C_{25}-S-10d_b-D-AC	26.73	1.17	25.90	5.728061
P-C_{25}-S-10d_b-D-AC	25.07			
P-C_{25}-S-15d_b-D-AC	30.52	0.52	30.15	4.445329
P-C_{25}-S-15d_b-D-AC	29.78			
P-C_{35}-S-10d_b-D-AC	46.10	1.82	44.81	9.910209
P-C_{35}-S-10d_b-D-AC	43.52			
P-C_{25}-S-10d_b-W-AC	24.60	1.45	23.57	5.212757
C-C_{25}-S-10d_b-W-AC	22.54			
C-C_{25}-G-5d_b	29.05	3.73	26.41	11.68171
C-C_{25}-G-5d_b	23.77			
C-C_{25}-G-15d_b	58.48	2.80	56.50	8.330385
C-C_{25}-G-15d_b	54.51			
C-C_{25}-G-10d_b	40.98	2.23	34.1	7.541578
C-C_{25}-G-10d_b	37.83			
C-C_{25}-S-15d_b	57.64	2.51	55.87	8.237497
C-C_{25}-S-15d_b	54.09			
C-C_{25}-S-10d_b	40.55	6.19	36.17	7.999381
C-C_{25}-S-10d_b	31.79			

4.1. Influence of Embedded Length on Post-Installed GFRP Reinforcement

When the embedded length is 5d, post-installed GFRP bars exhibit optimal bonding performance, achieving a pull-out load of 2209 with adhesive A, indicating a uniform stress distribution. Moreover, (Fig. 5a). shows that bond strength does not increase proportionally as the embedded length increases. This is due to the nonlinearity in the distribution of stress. The bond strength value using adhesive A is 2.6% and 40.3% higher than that obtained with adhesive B and adhesive

C, respectively. Furthermore, as shown in (Fig. 5a), when the embedded length is increased to 10d and 15d, the hierarchical arrangement of the three adhesives remains consistent with that obtained with the shorter embedded length (5d). However, the incremental rate of the bonding strength increase differs; Adhesive A exhibits bond strength 19.3% and 33.9% higher than adhesive B and adhesive C, respectively, when the embedded length is increased from 5d to 10d. Additionally, when the embedded length increases from 10d to 15d, adhesive A maintains optimal bonding performance, with bond strength increases of 43.2 % and 75.2% compared to adhesive B and adhesive C, respectively.

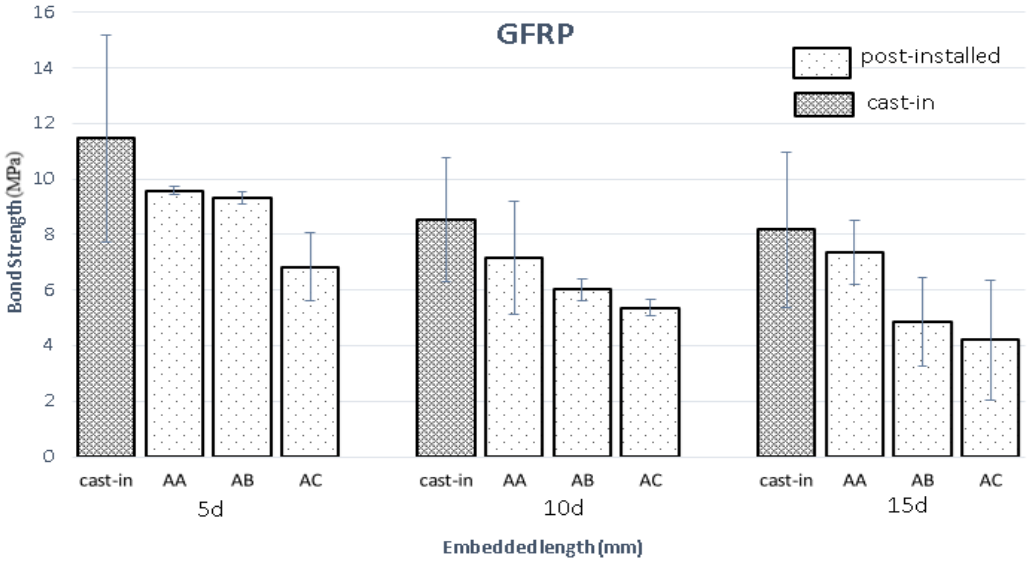

(a)

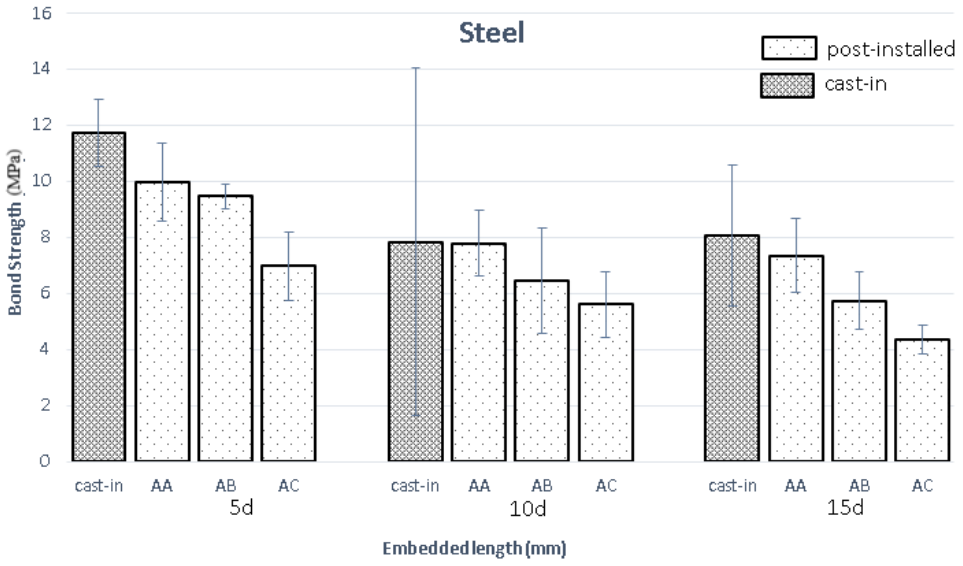

(b)

Fig. 5. Bond stress versus embedded length: (a) GFRP bars; (b) Steel bars

4.2 Influence of Embedded Length on Cast-In GFRP Reinforcement

Utilizing adhesive A at 5d,10d, and 15d embedded lengths, the bonding strengths of the post-installed bars were 83.6%, 89.1%, and 90%, respectively, when compared to the cast-in-place bonding strength at the same embedded lengths, see Fig. 5a. For adhesive B, the bonding strengths at 5d,10d, and 15d embedded lengths were 81.4%, 70.3%, and 62.8%, respectively, of the cast-in-place bonding strength. Similarly, for adhesive C, the bonding strengths at 5d,10d, and 15d embedded lengths were about 59.5%, 62.6%, and 51.3%, respectively, of the cast-in-place bonding

strength. This leads to the observation that cast-in GFRP has superior bonding with longer embedding lengths, given that fresh concrete provides better confinement than post-installed adhesives.

4.3 Influence of Compressive Strength on GFRP Reinforcement

For the stronger concrete cylinders, the bond strength is significantly improved. For example, utilizing GFRP rebars increases the bond strength of higher-strength concrete (i.e., 35 MPa) by 19.45 %, 11%, and 5.3% for specimens with 10d embedment lengths utilizing adhesives A, B, and C, respectively, compared to regular-strength concrete (i.e., 25 MPa). This leads to the conclusion that bond strength is augmented with rising compressive strength due to enhanced mechanical interlock.

4.4 Influence of Wet Environment on GFRP Reinforcement

The bond strengths of all applied adhesives decrease in a wet environment due to the adhesives' sensitivity to surface moisture. declined by 20.5%, compared to 15.9 % for adhesive B and 13.6% for Adhesive A. The bond strength of adhesive C is more significantly impacted due to its higher sensitivity to moisture. Still, in a wet environment, adhesive A exhibits the strongest bonding strength for GFRP bars in wet conditions.

4.6 Influence of Embedded Length on Post-Installed Steel Reinforcement

As shown in Figure 5b, adhesive A with a bond strength of 10.17 MPa performs best at 5d embedded length. Adhesive B and adhesive C have 5% and 30% lower bond strengths. Even at 10d and 15d embedded lengths, the three adhesives' hierarchical arrangement is similar to that of 5d. Moreover, adhesive A exhibits a 20.7% and 38.8% greater incremental rate of bond strength increase than adhesive B and adhesive C, respectively, when the embedding length is increased from 5d to 10d adhesive A exhibits the most effective bonding performance when the embedding length extends from 10d to 15d since the bond strength increases by 44.8%, 27.9%, and 16.4%, respectively, when employing adhesives A, B, and C. The results illustrate that adhesive A is the most effective adhesive that can be used with long-embedded steel rebars.

4.6 Influence of Embedded Length on Cast-In on Steel Reinforcement

The bond strengths at embedded lengths of 5d, 10d, and 15d for adhesive A were 81.8%, 99.3%, and 95.2% of the cast-in-place bond strength, respectively, see Fig. 5b. Comparing adhesive C to the cast-in-place bond strengths, the corresponding bond strengths at 5d, 10d, and 15d were about 77.7%, 82.3%, and 71.1%, respectively. Bond strengths for adhesive C at the same embedded lengths were about 57.29%, 71.6%, and 53.9% of the bond strengths for the cast-in-place method, respectively. This indicates that the relationship between the embedded length and the bonding strength of the bar to the concrete becomes nonlinear at longer embedded lengths.

4.7 Influence of Compressive Strength on Steel Reinforcement

Steel bars in concrete cylinders with higher compressive strength bond more effectively. In Table 7, higher-strength concrete (35 MPa) improves the bond strength of post-installed steel rebar by 23.1%, 13.7%, and 73% for specimens with 10d embedment lengths using adhesives A, B, and C, respectively, compared to regular concrete (25 MPa). In a high compressive strength scenario, adhesive C has a bonding strength of 9.91 MPa, slightly higher than adhesive A's 9.78 MPa. This shows that adhesive C with high concrete compressive strength improves structural performance by slowing the formation of concrete splitting cracks; moreover, it is cost-effective.

4.8 Influence of Wet Environment on Steel Reinforcement

Adhesive C shows that steel bars post-installed into wet holes had a 10.39% reduced bonding strength of 5.21 MPa than specimens with dry holes (Table 7). Adhesive A specimens have a bonding strength of 6.99 MPa and a 13.6% reduction, while adhesive B specimens have a 16.28% reduction. This clearly demonstrates that moist surfaces function as a barrier and diminish adhering performance.

4.9 Failure Modes

None of the specimen samples failed by pull-out; however, all split the concrete as shown in Figures 6 and 7. Concrete splitting occurs because the concrete surrounding the rebar cannot withstand the circumferential (hoop) tensile stresses resulting from radial pressure along the bond interface [23,24]. This failure usually occurs on the concrete surface and spreads along the rebar. Figure 7 illustrates the failure modes of concrete cylinders, where the splitting cracks terminate at the tips of embedded bars. Specimens with shorter embedded lengths had localized splitting cracks near the loaded end, whereas those with longer embedded lengths exhibited extended splitting cracks proportional to the embedded length.. The absence of pull-out failure indicates that epoxy resins are effective bonding agents and can be used to rehab reinforced concrete structures [25].

Fig. 6. failure modes of the examined specimens

(a) (b) (c)

Fig. 7. Effect of embedded length on concrete splitting failure. (a) le=5d, (b) le=10d, and (c) le=15d

5. Conclusions

- The most significant parameter influencing bonding strength is the embedded length of the bars. At shorter embedded lengths, the difference in bonding strength among various adhesions is minimal, but this difference increases as the bars' length increases.
- Adhesive A and adhesive B demonstrated comparable bonding at shorter GFRP and steel rebar embedding lengths, with adhesive A being 2.6% and 5% stronger, respectively.

However, as embedded length increased, the difference between the adhesives became more pronounced, regardless of bar type.

- Post-installed GFRP bars achieved 83- 90% of the bond strength of cast-in samples. While steel bars ranged from 81-99%. Unlike GFRP bars, Steel bars exhibit nonlinearity in the incremental rise of bonding strength as embedded length increases, especially at longer embedded lengths.
- Increasing concrete compressive strength enhanced bond strength by 5-19% for GFRP as well as 13-73% for steel. Adhesive C excelled in steel, whereas adhesive A excelled in GFRP, due to its higher stiffness and optimal curing characteristics.
- The insertion of rebars in wet holes reduced bonding strength by up to 20.5% for GFRP bars in addition to 16.28% for steel, with the greatest decline seen with adhesive C in GFRP applications. This significant reduction in bond strength is attributed to the adhesive's sensitivity to surface moisture, which hinders bonding to the concrete surface and decreases mechanical interlock.
- Splitting and crushing of concrete cylinders have been the main failure mechanisms. This shows that the rebar-concrete interface bond strength surpasses the concrete cylinder tensile stress. Yet, it is weaker than the bars' tensile strength. GFRP bars achieved adequate post-installed bond behavior. As a result, GFRP bars are suitable as an alternative replacement for steel bars in corrosive environments.
- Further studies are recommended to investigate the effects of harsh environmental conditions and higher compressive strengths on bonding strength to provide a better comprehension of performance under various conditions.

References

[1] El Refai F, Abed A, Altalmas A. Bond Durability of Basalt Fiber-Reinforced Polymer Bars Embedded in Concrete under Direct Pullout Conditions. J Compos Constr. 2015 Oct;19(5). https://doi.org/10.1061/(ASCE)CC.1943-5614.0000544

[2] Yan F, Lin Z, Yang M. Bond mechanism and bond strength of GFRP bars to concrete: A review. Compos B Eng. 2016 Aug;98:56-69. https://doi.org/10.1016/j.compositesb.2016.04.068

[3] Cook RA, Kunz J, Fuchs W, Konz RC. Behavior and design of single adhesive anchors under tensile load in uncracked concrete. ACI Struct J. 1998 Jan 1;95(1):9-26. doi: 10.14359/522. https://doi.org/10.14359/522

[4] Cook RA. Behavior of chemically bonded anchors. J Struct Eng. 1993 Sep;119(9):2744-62. https://doi.org/10.1061/(ASCE)0733-9445(1993)119:9(2744)

[5] Mahrenholtz C, Eligehausen R, Reinhardt HW. Design of post-installed reinforcing bars as end anchorage or as bonded anchor. Eng Struct. 2015;100:645-55. https://doi.org/10.1016/j.engstruct.2015.06.028

[6] Tayeh BA, EL dada ZM, Shihada S, Yusuf MO. Pull-out behavior of post installed rebar connections using chemical adhesives and cement based binders. J King Saud Univ Eng Sci. 2019 Oct;31(4):332-9. https://doi.org/10.1016/j.jksues.2017.11.005

[7] Wang D, Wu D, Ouyang C, Zhai M. Performance and design of post-installed large diameter anchors in concrete. Constr Build Mater. 2016 Jul;114:142-50. https://doi.org/10.1016/j.conbuildmat.2016.03.167

[8] Hamad BS, Al Hammoud R, Kunz J. Evaluation of bond strength of bonded-in or post-installed reinforcement. ACI Mater J. 2006;103(2):207. https://doi.org/10.14359/15178

[9] Cosenza E, Manfredi G, Realfonzo R. Behavior and Modeling of Bond of FRP Rebars to Concrete. J Compos Constr. 1997 May;1(2):40-51. https://doi.org/10.1061/(ASCE)1090-0268(1997)1:2(40)

[10] Veludo J, Júlio ENBS, Dias-Da-Costa D. Compressive strength of micropile-to-grout connections. Constr Build Mater. 2012 Jan;26(1):172-9. doi: 10.1016/j.conbuildmat.2011.06.007. https://doi.org/10.1016/j.conbuildmat.2011.06.007

[11] ACI Committee 408. 408R-03: Guide for Design and Construction of Externally Bonded FRP Systems for Strengthening Concrete Structures. Farmington Hills, MI: American Concrete Institute; 2003.

[12] ACI Committee 355.1R-91: State-of-the-Art Report on Bonding of In-Place Reinforcement and Post-Installed Reinforcement. Farmington Hills, MI: American Concrete Institute; 1991.

[13] Tastani SP, Pantazopoulou SJ, Asce M. Bond of GFRP Bars in Concrete: Experimental Study and Analytical Interpretation. J Compos Constr. 2006 Oct;10(5):381-91.

[14] Pecce M, Manfredi G, Realfonzo R, Cosenza E. Experimental and Analytical Evaluation of Bond Properties of GFRP Bars. J Mater Civ Eng. 2001 Aug;13(4):282-90. https://doi.org/10.1061/(ASCE)0899-1561(2001)13:4(282)

[15] Kim B, Doh JH, Yi CK, Lee JY. Effects of structural fibers on bonding mechanism changes in interface between GFRP bar and concrete. Compos B Eng. 2013 Feb;45(1):768-79. https://doi.org/10.1016/j.compositesb.2012.09.039
[16] ASTM International. ASTM A706/A706M: Standard Specification for Deformed and Plain Low-alloy Steel Bars for Concrete Reinforcement. West Conshohocken, PA: ASTM; 2015.
[17] ASTM International. ASTM C127: Standard Test Method for Density, Relative Density (Specific Gravity), and Absorption of Coarse Aggregate. West Conshohocken, PA: ASTM; 2021.
[18] ASTM International. ASTM C128: Standard Test Method for Density, Relative Density (Specific Gravity), and Absorption of Fine Aggregate. West Conshohocken, PA: ASTM; 2022.
[19] ASTM International. ASTM C29/C29M: Standard Test Method for Bulk Density (Unit Weight) and Voids in Aggregate. West Conshohocken, PA: ASTM; 2023.
[20] ASTM International. ASTM C136/C136M: Standard Test Method for Sieve Analysis of Fine and Coarse Aggregates. West Conshohocken, PA: ASTM; 2021.
[21] ACI Committee 211. ACI 211.1: Standard Practice for Selecting Proportions for Normal, Heavyweight, and Mass Concrete. Farmington Hills, MI: American Concrete Institute; 2022.
[22] ACI Committee 440. 440.3R-04: Guide Test Methods for Fiber-Reinforced Polymers (FRPs) for Reinforcing or Strengthening Concrete Structures. Farmington Hills, MI: American Concrete Institute; 2004.
[23] Agarwal J. Bond behavior of post-installed Glass fiber reinforced polymer (GFRP) rebars [dissertation]. West Lafayette (IN): Purdue University;2023.
[24] Mutashar BM, Salih OA, Kasim SY. A Review of the Bond Mechanism and Bond Strength of Fiber Reinforced Polymer Rebars to Concrete. Misan Journal of Engineering. 2025 Feb 19:29-45.
[25] Ahmed KS, Shahjalal M, Siddique TA, Keng AK. Bond strength of post-installed high strength deformed rebar in concrete. Case Stud Constr Mater. 2021 Dec;15. https://doi.org/10.1016/j.cscm.2021.e00581